Available online at www.sciencedirect.com
SCIENCE DIRECT®
Journal of Nuclear Materials 325 (2004) 18–25
journal of nuclear materials
www.elsevier.com/locate/jnucmat

Thermal expansion studies on Inconel-600® by high temperature X-ray diffraction ☆

S. Raju [a,*], K. Sivasubramanian [b], R. Divakar [a], G. Panneerselvam [c], A. Banerjee [a], E. Mohandas [a], M.P. Antony [c]

[a] *Materials Characterisation Group, Physical Metallurgy Section, Indira Gandhi Centre for Atomic Research, Kalpakkam 603 102, India*
[b] *Engineering Safety Division, Indira Gandhi Centre for Atomic Research, Kalpakkam 603 102, India*
[c] *Fuel Chemistry Division, Indira Gandhi Centre for Atomic Research, Kalpakkam 603 102, India*

Received 28 July 2003; accepted 23 October 2003

Abstract

The lattice thermal expansion characteristics of Inconel-600® have been studied by high temperature X-ray diffraction (HT-XRD) technique in the temperature range 298–1200 K. Altogether four experimental runs were conducted on thin foils of about 75–100 μm thickness. The diffraction profiles have been accurately calibrated to offset the shift in 2θ values introduced by sample buckling at elevated temperatures. The corrected lattice parameter data have been used to estimate the instantaneous and mean linear thermal expansion coefficients as a function of temperature. The thermal expansion values estimated in the present study show a fair degree of agreement with other existing dilatometer based bulk thermal expansion estimates. The lattice parameter for this alloy at 300 K is found to be 0.3549(1) nm. The mean linear thermal expansivity is found to be 11.4×10^{-6} K^{-1}.

1. Introduction

A knowledge of thermal expansion characteristics of a material is of importance in both basic and applied contexts. The fact that thermal expansion arises as a consequence of lattice anharmonicity, makes it a key quantity in fundamental studies on cohesive forces. On the applied front, the availability of critically evaluated thermal expansion data is essential in drafting proper design specifications of the concerned material in technologically demanding applications. It is in this perspective, that the present study is concerned with the accurate determination of the thermal expansion characteristics of a commercially important alloy, namely, Inconel-600®. This material is a fairly common nickel base solid solution alloy, containing chromium, iron and carbon as the principal alloying additions (Table 1). Inconel-600® is rather well known for its corrosion resistance against acids at moderate temperatures [1]. Besides, it is also used somewhat less extensively in certain critical applications in nuclear reactors [2].

In fact, the present study is made on an Inconel-600® alloy, that is used to form the annular ring separating the two pole-pieces of the electromagnet of the diverse safety rod drive mechanism (DSRDM) of India's first 500 MW(e) prototype fast breeder reactor (PFBR). This Inconel-600® ring is welded on either side to soft-iron pole pieces by standard TIG welding procedure, using Inconel-82® as the filler wire [3]. The choice of Inconel-600® for this component is based mainly on two considerations. At the normal operating temperature of about 773 K (500 °C), Inconel-600® is non-magnetic in nature, and further, its thermal expansivity is not

☆ ® Inconel is a registered trademark of International Nickel Company.

* Corresponding author. Tel.: +91-4114 480306; fax: +91-4114 480081.
E-mail address: sraju@igcar.ernet.in (S. Raju).

0022-3115/$ - see front matter © 2003 Elsevier B.V. All rights reserved.
doi:10.1016/j.jnucmat.2003.10.007

Table 1
Nominal composition in wt% of Inconel-600® used in the present study

Element	Inconel-82®	Inconel-600®	Inconel-625®	Pyros
Ni (+Co)	72	72	59	82
C	0.02	0.15	0.1	
Mn	3.00	1	0.5	3
Fe	1.00	8	5	3
Si	0.20	0.5	0.5	
Cu	0.04	0.5		
Cr	20.0	15.5	21.5	8
Ti	0.55		0.4	
Nb (+Ta)	2.50		3.65	
S	0.007	0.015	0.015	
Mo			9	$W = 4$
Al			0.4	

For comparison, the composition of Inconel-82® filler wire, Inconel-625® and Pyros, another high nickel solid solution alloy are also listed.

drastically different from that of ASTM-A848-87-alloy 1 (Fe–0.35wt%Mn–0.05wt%C), that is used for making the electromagnet [3]. In this connection, it is obvious, that a serious mismatch in the thermal expansion characteristics of the respective metals constituting the dissimilar joint may give rise to thermal stresses at the weld interface. The onset of thermal stresses in excess of the design-limit, can over a period of time pave way for the impairment of the overall metallurgical integrity of the component itself. Therefore, reliable thermal expansion data on Inconel-600® is crucial from the point of view of ensuring a reliable design of the dissimilar weldment in DSRDM electromagnet [3,4]. Although, useful information on the mean linear thermal expansion coefficient of Inconel-600® could be gleaned from the open literature [1,5–8], we did not come across any detailed HT-XRD based thermal expansion study on this material. Inconel-600®, being a simple face centered cubic solid solution alloy, it is indeed possible to obtain an accurate estimate of thermal expansion by monitoring the change in its lattice dimension as a function of temperature. Further, the thermal expansion data obtained using HT-XRD would nicely complement the dilatometry based data, that are characteristic of bulk thermal expansion and are the frequently reported ones in technical literature. In this paper, we describe our HT-XRD studies on a commercial Inconel-600® alloy in the temperature range 298–1200 K. The experimental details are given below.

2. Experimental details

The Inconel-600® used in the present study was procured from M/s. Huntington Alloys Inc., in the form of a circular rod of about 3.5 cm in diameter. The nominal composition of this alloy as certified by the supplier is listed in Table 1, together with that of Inconel-82® filler wire used for welding these alloys. Thin slices were cut from this rod and were cold rolled to obtain foils of thickness, ranging from 75 to 100 μm. These foils were subsequently strain relieved by annealing them at 1323 K for about 30 min in argon atmosphere. The HT-XRD studies were performed in a Philips-X'pert MPD® system, equipped with Büehler's high vacuum heating stage. The heating stage consists of a thin (∼80 μm) resistance heated tantalum foil, on top of which the inconel sample is placed. The temperature is measured by a W–Re thermocouple, which is spot welded to the bottom of the tantalum heater. The temperature is controlled to an accuracy of about ±1 K. The specimen stage is flushed with high purity argon before the start of every experimental run and a general vacuum level of about 10^{-5} mbar is maintained throughout the experiment. Owing to the intrinsic design of the heating stage and also due to the residual non-planarity of our rolled foil sample, there prevails an unavoidable temperature drop at the heater–sample interface. In addition there is also present a temperature gradient across the section thickness of the sample. This temperature gradient may be minimised by using a thin foil, although too thin a foil results in buckling or sample geometry deformation at high temperatures. The diffraction studies were performed using CuK_α radiation in θ–θ geometry at a temperature interval of 50 K. A heating rate of 1 K min^{-1} and a holding time of 30 min at each temperature of measurement are adopted. The primary data acquisition cum preliminary analysis were performed by the Philips X'pert Pro® software, although at a latter stage, we resorted to an independent processing of the raw data for a precise determination of the peak position. The 2θ calibration for the room temperature (∼298 K) run is made with the help of silicon and α-alumina standards. However, for high temperatures, we resorted to co-recording of the XRD pattern of the tantalum heater foil together with sample reflections. This is made possible by cutting a very narrow key hole like wedge in the inconel sample, exposing thus a good amount of sample as well as the underlying tantalum heater surface to the incident X-rays. The experimentally obtained reflections for tantalum, vis-à-vis the recommended temperature dependent lattice parameter data, taken from the assessment of Wang and Reeber [9] have been used to calibrate the apparent shift introduced to the recorded 2θ values, due to sample geometry deformation. This procedure, however, does not yield any absolute, or for that matter, separable estimates of the total error in the recorded 2θ, as distinctly arising from the temperature difference between the heater foil and the sample and that due to sample distortion upon possible buckling at high temperature. By performing

altogether four runs on samples of slightly varying thickness, in the range 75–100 μm, in such a manner that, with two of the runs involving a concurrent recording of the reflections from the sample and tantalum, and with the other two recording only the sample reflections, we could estimate the correction to be made to the measured 2θ values to get the actual ones. As a final point, we would like to mention that every repeated XRD run performed on a specific sample resulted in quite reproducible results.

3. Results

In Fig. 1, the room temperature XRD profiles of as received, annealed and after HT-XRD scanned specimens are presented. Although, there is an overall agreement among these profiles, it could nonetheless be noticed that the peak positions exhibit a very small shift to higher 2θ values upon annealing. Further, it is also instructive to note that the sample after being subjected to continuous heating cum holding cycle that is inherent in our experimental schedule, reveals a much sharper peak, especially for the (2 2 0) reflection, as compared to that of the cold rolled specimen. While the relieving of strain accrued in the matrix as a result of cold work can contribute to the clear resolution of peak shapes, the reason behind the slight increase in lattice parameter that is evident upon ageing is not clear. It is quite likely that the onset of any precipitation process, in particular the initial stages of a precipitate nucleation involving a distinct structural rearrangement of the matrix at a spatial extent of a few lattice-spacings, might present itself as a gentle shift in the matrix reflection [10]. On the other hand, the formation of such fine precipitates can also cause a local compression of the soft nickel rich matrix, if the precipitate phase were to be hard or less compressible. This proposition is qualitatively in accord with the mild, but definite reduction in the matrix lattice parameter in the annealed state. The relative lattice parameter change as estimated by XRD is brought out in Table 2, where in we have listed the 2θ, and the lattice parameter (a) values corresponding to the three XRD profiles shown in Fig. 1.

In order to further verify this hypothesis, we performed a transmission electron microscopy (TEM) study of the X-ray scanned sample. The results are shown in Fig. 2. The samples for TEM are prepared by standard ion-milling technique. The details of microstructural characterisation will be published separately. In the present context, it is sufficient to note that the TEM study offers a clear-cut evidence for the presence of precipitates occurring both within the matrix and along the grain boundaries. An analysis of the selected area diffraction pattern obtained from the precipitate–matrix overlapping region indicates that these precipitates belong to both $M_{23}C_6$ and M_7C_3 type carbides. Since the volume fraction of these precipitates is rather small, their presence could not be detected in the XRD study. As the present paper is devoted to studying the thermal expansion characteristics, the development microstructural features upon ageing is not discussed here.

In Fig. 3, a stack of XRD profiles pertaining to different temperatures in the range 373–1273 K is presented.

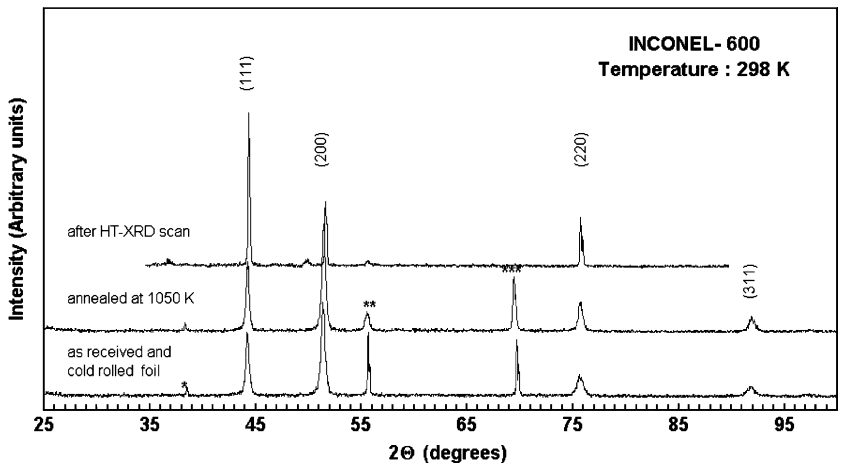

Fig. 1. The three XRD profiles obtained from Inconel-600® alloy, at three different conditions are stacked one over other with a pseudoshift along the Y-axis. In addition, the XRD patterns recorded on the as received and annealed specimens contain certain reflections arising from the reference tantalum foil. These reflections marked by asterisk (*: 1 1 0, **: 2 0 0, ***: 2 1 1) were co-recorded with the inconel ones for the purpose of calibration. The gradual shift in the inconel reflections upon annealing and ageing is worth noting. This is suggestive of some mild lattice compression brought upon by precipitation during the course of continued heating and thermal holds. Refer to text for details.

Table 2
Listing of 2θ and lattice parameter values for different (hkl) reflections recorded respectively for the cold rolled, solution annealed and HT-XRD scanned specimens

Run description	2θ values (radians)				a values for different (hkl) reflections (10^{-10} m)			
	(1 1 1)	(2 0 0)	(2 2 0)	(3 1 1)	(1 1 1)	(2 0 0)	(2 2 0)	(3 1 1)
As received & cold rolled	0.7712	0.8966	1.3198	1.6040	3.5470	3.5543	3.5537	3.5542
Annealed at 1323 K	0.7723	0.8976	1.3229	1.6047	3.5425	3.5504	3.5466	3.5530
After HT-XRD experiment	0.7740	0.9008	1.3224	Not recorded	3.5349	3.5388	3.5482	Not recorded

It can be seen that there is a mild but definite decrease in the lattice parameter upon strain relieving and subsequent prolonged heating and holding schedule carried out in situ in X-ray diffractometer. Refer to text for further details.

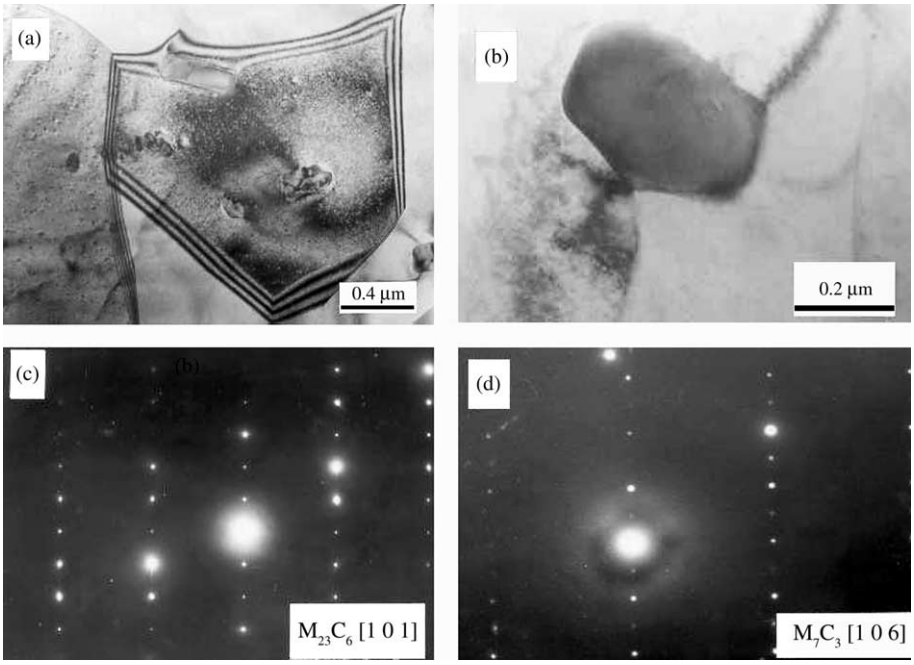

Fig. 2. Microstructure of the HT-XRD scanned Inconel-600® alloy obtained using transmission electron microscopy. In (a), the presence of precipitates well inside the fcc matrix as well at the grain boundary can be seen. In (b), a typical precipitate as seen in the bright field mode is shown. The selected area diffraction patterns (c&d) obtained from these precipitates suggest that these belong to $M_{23}C_6$ and M_7C_3-type carbides.

This is a typical HT-XRD run made with 100 μm thick foil. The lattice parameter (a) is estimated from the three major fcc reflections, namely, (1 1 1), (2 0 0) and (2 2 0). Finally an effective high angle corrected lattice parameter at each temperature is obtained by the standard Nelson–Riley extrapolation procedure [11].

In Fig. 4, the lattice parameter data as a function of temperature for four individual runs taken with foils of slightly varying thickness are plotted. Admittedly there is certain amount of scatter among the data obtained in the four runs. As mentioned earlier, one possible reason for this could be the varying amount of sample buckling, besides the temperature difference prevailing at the sample–heater interface. The thinner foil, for obvious reasons experiences a minimal temperature gradient across its section thickness, and hence, is more close to the actual heater temperature. But the problem with the thin foil is that at high temperatures, it tends to deform

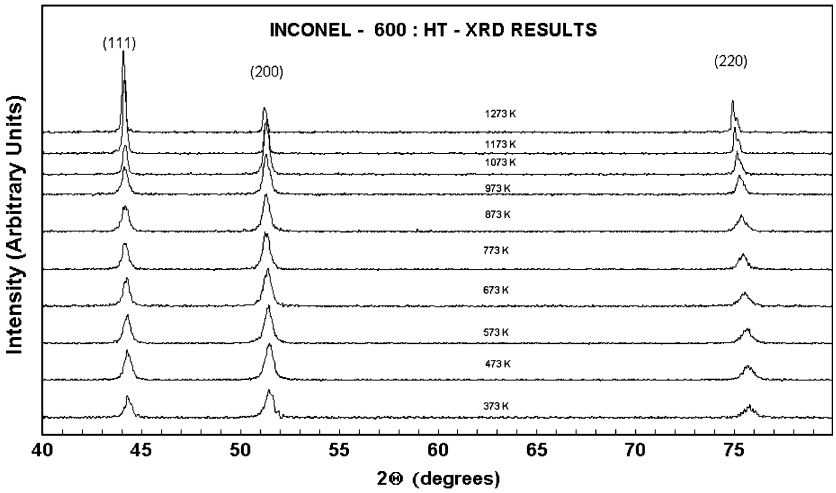

Fig. 3. A collage of HT-XRD profiles corresponding to different temperatures is presented. Note that the reference tantalum reflections are stripped in these patterns for enhancing clarity.

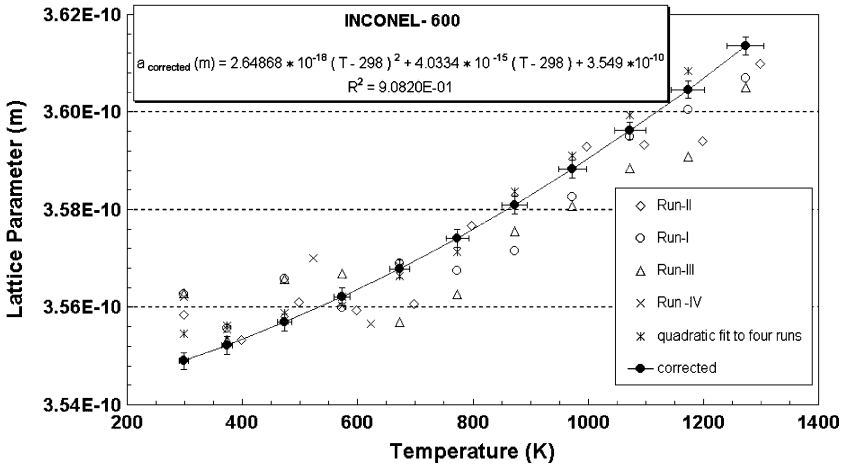

Fig. 4. The temperature dependence of the lattice parameter data is graphically illustrated.

rather easily and introduces a distortion of the diffraction geometry. The extent of this sample geometry distortion induced shift in 2θ is a very difficult issue to be quantified in rigorous terms. As a simple remedy, we fitted all the data coming from samples of varying thickness to a second degree polynomial in temperature increment (T-298) and corrected the resulting best fit data using the co-recorded tantalum reflections. This calibration method relied on the assumption that the apparent errors in the measured 2θ behaved identically for both tantalum and the sample. Although lacking in sophistication, this procedure yielded a fair amount of success in our recent thermal expansion studies on D9-stainless steel and Inconel-82® filler wire [12,13]. It was estimated that an uncertainty of ±25 K in temperature resulted in a change of lattice parameter of about ±0.00275 nm for $T \geqslant 800$ K. At lower temperatures, the error is much less. The relative error in 2θ measurement is calibrated at room temperature by using silicon and α-alumina standards. As mentioned before, the data from all the four runs were made use of in estimating the precision in the lattice parameter. The corrected lattice parameter data thus obtained are displayed in Fig. 4.

For the purpose of calculating thermal expansivity, the corrected lattice parameter variation with temperature (K) is fitted to a second-degree polynomial in the temperature increment (T-298):

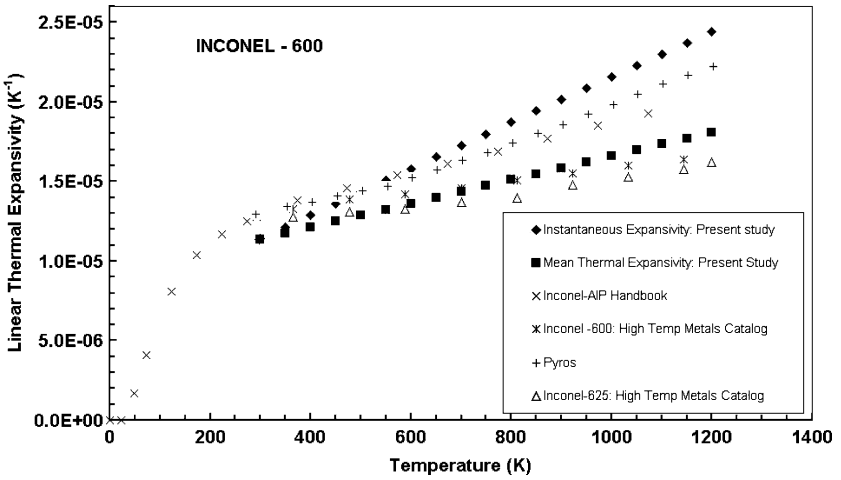

Fig. 5. The instantaneous and mean linear thermal expansivity values obtained in the present study are graphically illustrated together with literature data on some inconel and related high nickel content alloys.

$$a_{\text{corrected}}\ (\text{m}) = 3.549 \times 10^{-10} + 4.033 \times 10^{-15}\ (T\text{-}298) + 2.6487 \times 10^{-18}\ (T\text{-}298)^2. \quad (1)$$

Once the lattice parameter is known as a function of temperature, it is then possible to estimate the instantaneous (α_L-instantaneous), mean (α_L-mean) and relative linear thermal expansion coefficients (α_L-relative) by the following relations:

$$(\alpha_L\text{-instantaneous}) = (1/a_T) \times (\mathrm{d}a_T/\mathrm{d}T), \quad (2)$$

$$(\alpha_L\text{-relative}) = (1/a_{298}) \times (\mathrm{d}a_T/\mathrm{d}T), \quad (3)$$

$$(\alpha_L\text{-mean}) = (1/a_{298}) \times \{(a_T - a_{300})/(T\text{-}298)\}. \quad (4)$$

Table 3
The lattice parameter as a function of temperature, instantaneous (α_L-instantaneous), mean (α_L-mean) and relative linear thermal expansivities (α_L-relative) for Inconel-600® estimated in the present study using HT-XRD are listed

T (K)	a (10^{-10} m)	a-corrected (10^{-10} m)	α_L-instantaneous (10^{-5} K^{-1})	α_L-mean (10^{-5} K^{-1})	α_L-relative (10^{-5} K^{-1})
298	3.5490	3.5490	1.14	–	1.14
300	3.5491	3.5491	1.14	1.14	1.14
350	3.5509	3.5512	1.21	1.18	1.21
400	3.5528	3.5534	1.29	1.21	1.29
450	3.5549	3.5557	1.36	1.25	1.36
500	3.5570	3.5582	1.43	1.29	1.44
550	3.5593	3.5609	1.51	1.32	1.51
600	3.5617	3.5636	1.58	1.36	1.59
650	3.5642	3.5665	1.65	1.40	1.66
700	3.5668	3.5695	1.73	1.44	1.74
750	3.5695	3.5726	1.80	1.47	1.81
800	3.5724	3.5759	1.87	1.51	1.89
850	3.5753	3.5793	1.94	1.55	1.96
900	3.5784	3.5829	2.02	1.59	2.04
950	3.5816	3.5866	2.09	1.62	2.11
1000	3.5849	3.5904	2.16	1.66	2.18
1050	3.5883	3.5943	2.23	1.70	2.26
1100	3.5919	3.5984	2.30	1.74	2.33
1150	3.5955	3.6026	2.37	1.77	2.41
1200	3.5993	3.6069	2.44	1.81	2.48

The lattice parameter values listed here correspond to corrected ones and are represented by Eq. (1) in the text. This is based on data obtained from four distinct XRD runs made on samples of different foil thickness. Refer to text for details.

In Fig. 5, we present the mean and the instantaneous linear thermal expansivity estimates obtained in the present study. These values are also listed in Table 3. For the sake of comparison, we also report in Fig. 5, the mean thermal expansivity values taken from a commercial catalogue [8] and those listed in the American Institute of Physics (AIP) handbook for a generic inconel alloy [5]. Although no experimental details could be obtained from these sources, it is likely that the quoted values might have been obtained using bulk samples in a dilatometer.

4. Discussion

At the outset, it must be mentioned that to the best of our knowledge, we are not aware of any other HT-XRD based thermal expansion estimate for Inconel-600®. Therefore it is not possible to make a direct assessment of the relative accuracy of present values in the light of similar literature data. However, the lattice parameter at 300 K obtained in the present study, namely 0.3549(1) nm, compares favourably with the value of 0.35402 nm, estimated by Müller and Schulze using XRD for a nickel base alloy of nominal composition (wt%) 73Ni–21.1Cr–5.9Fe [14]. The same study also mentions the fact that the lattice parameters of ternary Ni–Cr–Fe alloys are generally sensitive to quenching and subsequent prolonged annealing heat treatments. Although, Inconel-600® is regarded as a non-precipitation hardenable alloy, the presence of carbon of about 0.15 wt% (see Table 1), and coupled to the fact that nickel evinces a little or almost nil solubility for carbon [15], it is very much possible that precipitation of some carbides is bound to occur during annealing at favoured nucleation sites like grain boundaries. The TEM micrographs shown in Fig. 2, clearly attest to the presence of carbide precipitates in well annealed samples.

By the way of comparison, we may note from Fig. 5 that the XRD based thermal expansivity estimates for Inconel-600® obtained in the present study are, by and large, in reasonable agreement with the general pattern exhibited by other similar nickel base alloys [16,17]. In specific terms, it emerges that our mean linear thermal expansivity values are slightly, but systematically lower than the AIP-handbook recommended ones [5]. This is understandable in the light of the fact that the selected values in this handbook are most likely to be dilatometric estimates [5]. At this juncture, a brief comparison of the two diverse methods of thermal expansion measurement, namely, the X-ray based absolute thermal expansion and the macroscopic length change measurements based on dilatometric technique, may be useful in assessing present results in an overall perspective. It is well known that X-ray method with proper calibration while capable of giving very accurate results does not however take into account the defect contribution to thermal expansion. This limitation becomes crucial while studying ceramic samples that are known to suffer from porosity, besides possessing appreciable non-stoichiometry. As for metallic alloys porosity is not a critical issue at all and further, the role of point defect induced excess contribution to thermal expansion assumes significance only at temperatures close to melting point. In view of this, it must be kept in mind that dilatometry based thermal expansion values are normally higher than that of X-ray based ones. In fact, the difference between the two may be used to obtain a measure of the defect concentration in an, otherwise porosity free samples [18]. The other point is that dilatometry performed over polycrystalline samples with non-cubic crystal structure offers only an average or effective thermal expansion; this limitation can however be overcome by using suitably oriented bulk single crystal specimens in place of polycrystalline rods. The powder diffraction on the other hand can provide very accurate information about the anisotropy of thermal expansion along different crystallographic directions. In a similar vein, we may also note that in case of samples containing more than one phase, dilatometry presents only an average of thermal expansion response of various constituting phases. The XRD technique on the other hand gives the actual dimensional change of individual phases concerned, if they are present in fairly adequate amount to register distinct reflections in the X-ray diffraction profile. The problem of eliciting a suitably averaged bulk thermal expansion value from individual phase specific linear thermal expansivities is a non-trivial issue. It is probably for this reason that macroscopic length change measurements are often preferred in material property data specification of many commercial multiphase alloys.

As for a comparison of the relative uncertainties in the two disparate techniques are concerned, it is rather a difficult issue to be assessed in rigorous terms. By employing sophisticated transducing techniques such as optical interferometry, capacitance change measurement, high speed photographic technique etc., and accompanied by recommended calibration procedures, modern dilatometric techniques rival the X-ray method in accurately estimating the temperature induced dimensional change [19,20]. In HT-XRD, the intrinsic poor quality of X-ray diffraction profiles recorded at high temperatures and also the difficulty associated with the precise temperature calibration contribute to a lowering of the intrinsic high accuracy of the thermal expansion measurement.

Now, judging our XRD based thermal expansion values on Inconel-600® in the light of the aforementioned comments, the following conclusions may be made. Considering the fact that the highest temperature reached in the present study (1200 K) is well below the melting point, the correction to measured thermal expansion arising from defect contribution is expected to be small.

Further, the presence of hard matrix and grain boundary precipitates may serve to further lower the thermal expansion. So there is every reason to believe that the present thermal expansion estimates are lower than the dilatometry based bulk values. By the way of comparing the present thermal expansion estimate with the values cited in the data sheet of High Temperature Metals Inc., [8], we note that our estimates are quantitatively similar; but differs qualitatively in the temperature variation. Besides, it may also be mentioned that in comparison with the reported data on other high nickel alloys like Inconel-625® [16] and Pyros [17], the present thermal expansion estimates for Inconel-600®, are of similar and expected order. However, based on our previous experience in studying the thermal expansion characteristics of stainless steels and other alloys we believe that the present estimates are accurate to with in ±5% [12,13].

5. Conclusion

The thermal expansion characteristics of Inconel-600® have been estimated by measuring accurately the temperature variation of lattice parameter in the temperature range 298–1200 K.

Acknowledgements

We thank Mrs R. Vijayashree and Mr V. Rajan Babu, for bringing this problem to our notice and also for the provision of the details of the DSRDM electromagnet assembly. The metallurgical aspects concerned with the welding procedure of dissimilar metals and other general information on inconel alloys were provided to us by Dr V. Shankar. The sustained encouragement and support that we received from Dr M. Vijayalakshmi, Dr V.S. Raghunathan, Dr P.R. Vasudeva Rao and Dr Baldev Raj, during the course of this work are sincerely acknowledged.

References

[1] Source Book on Industrial Alloy and Engineering Data, ASM Metals Park, OH, 1972, p. 312.
[2] S.L. Mannan, S.C. Chetal, Baldev Raj, S.B. Bhoje, Trans. Ind. Inst. Metals 56 (2003) 155.
[3] R. Vijayashree, Drg. No.: PFBR/31440/DD/1540/R-3, IGCAR internal report, 2003.
[4] V. Shankar, H.C. Dey, IGC/MTD/MJS/2003/02, IGCAR internal report, 2003.
[5] D.E. Gray, American Institute of Physics Handbook, 3rd Ed., McGraw-Hill Book Company, New York, 1972, p. 4.
[6] V. Arp, J.H. Wilson, L. Winrich, P. Sikora, Cryogenics 2 (1962) 230.
[7] A.F. Clark, Cryogenics 8 (1968) 282.
[8] The supplier's catalogue of M/s. High Temp Metals Inc., available from <http://www.hightempmetals.com/>.
[9] K. Wang, R.R. Reeber, Mater. Sci. Engg. (Reports) R 23 (1998) 101.
[10] H. Jones, in: F.H. Chung, D.K. Smith (Eds.), Industrial Applications of X-ray Diffraction, Marcel-Decker, New York, 2000, p. 129.
[11] B.D. Cullity, Elements of X-ray Diffraction, 2nd Ed., Addison Wesley Publishing Company, Reading, MA, 1978, Chapter 11.
[12] R. Jose, S. Raju, R. Divakar, E. Mohandas, G. Panneerselvam, M.P. Antony, K. Sivasubramanian, J. Nucl. Mater. 317 (2003) 54.
[13] G. Panneerselvam, S. Raju, R. Jose, R. Divakar, E. Mohandas, K. Sivasubramanian, M.P. Antony, Mater. Lett. 58 (2003) 216.
[14] H.-G. Müller, H.A. Schulze, Z. Metallk. 48 (1957) 48; as cited by W.B. Pearson, in: Handbook of Lattice Spacings of Metals and Alloys, vol. II, Pergamon, London, 1958.
[15] T.B. Massalski, P. Okamoto, P.R. Subramanian, L. Kacprazak (Eds.), ASM Binary Alloy Phase Diagram, vol. 1, 2nd Ed., ASM International, Materials Park, OH, 1990, p. 866.
[16] The supplier's catalogue for Inconel-625® from M/s. High Temp Metals Inc., available from <http://www.hightemp-metals.com/>.
[17] C.A.V. de Rodrigues, G. Cizeron, Int. J. Thermophys. 6 (1985) 715.
[18] R.O. Simmons, R.W. Balluffi, Phys. Rev. 119 (1960) 600.
[19] A.P. Miller, A. Cezairliyan, in: C.Y. Ho (Ed.), Thermal Expansion of Solids, CINDAS Data Series on Material Properties, ASM International, Materials Park, OH, 1998, p. 243.
[20] C.A. Swenson, in: C.Y. Ho (Ed.), Thermal Expansion of Solids, CINDAS Data Series on Material Properties, ASM International, Materials Park, OH, 1998, p. 207.